NON-LINEAR PHASE SPACE TUNING FOR IN-FLIGHT FRAGMENT SEPARATORS

D. Kallendorf*[1,2], A. Andres[2], S. Appel[2], M. Bajzek[2], J. Hetzel[2], V. Isensee[1,2], E. Kazantseva[2], P. Madysa[2], S. Pietri[2], H. Weick[2], J. Wirtz[2,1]
[1]Technical University of Darmstadt, Darmstadt, Germany
[2]GSI Helmholtz Centre for Heavy Ion Research, Darmstadt, Germany

Abstract

Next generation in-flight fragment separators like the Super-FRS are built with large apertures to accept high momentum spreads. The wide beam and momentum variation gives rise to large aberrations from non-linear effects, if not suppressed precisely. Models and simulations are able to predict most effects, but to achieve the highest performance, fine tuning of the ion optics with beams, based on measured aberrations for the machine is needed.

While the main focal planes provide single particle tracking to measure the phase space, the target area instrumentation can only provide coarse information about the overall distribution of the beam. This poses a challenge, as knowledge about the polynomial order of the phase space distortion (in terms of transfer maps) enables a much faster optimization.

In this setting, we used a normalizing-flow-like approach, to find an invertible symplectic kick-rotation-* map, which transforms the measured data into an initial distribution, to extract a possible transfer-map and determine the distortions by order.

Integrated in the Generic Optimisation Frontend and Framework (Geoff), the method was validated in simulations and with a multiple charge state uranium beam at GSI's fragment separator (FRS), by fine-tuning even significantly detuned optics.

TRANSFER MAPS

The main scope of day-to-day beam-line tuning is alignment and focus of beams by means of dipole and quadrupole magnets. In case of small beam emittances and small apertures, linear optics can be used to describe the transformation of normally distributed beam, whereas the transformations are applied to the stochastic mean and covariance of the beam distribution. While knowledge of these stochastic momenta is still valuable for the fragment separators, the nonlinearities in dipoles and quadrupoles lead to their wrong characterization when linear transformations are used to describe the system, as illustrated in Fig. 1a.

The transfer map description is a powerful tool to describe non-linear effect in accelerators, by expressing the final particle coordinates as polynomial $\mathcal{T}$ of the initial coordinates. The coefficients of the polynomial, called transfer map coefficients can give insight into the beam dynamics and are notated in short-form as $(x_\mathrm{f}^i|x_\mathrm{i}^j)$ for the first order

* d.kallendorf@gsi.de

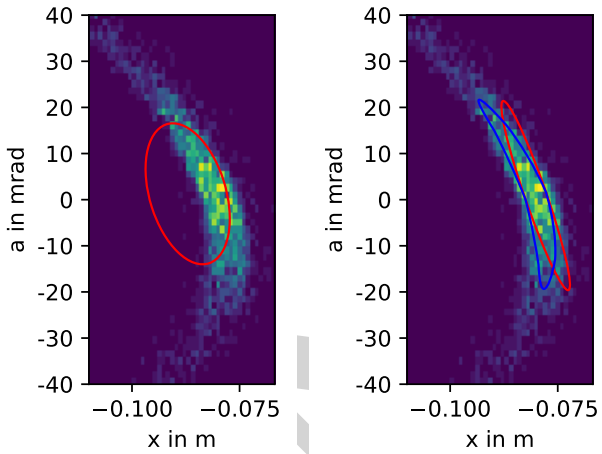

(a) Linear phase space (red) from mean and covariance

(b) Linear (red) and quadratic (blue) phase space from generalized Irwin model.

Figure 1: Determining beam properties from a simulated quadratic distorted phase space.

and $(x_\mathrm{f}^i|x_\mathrm{i}^j x_\mathrm{i}^k)$ for the second order, such that final coordinate x_f^i has this coefficient for the respective monomial in the initial coordinates. In the rare case that the full phase space coordinates before and after a section are available, this polynomial can be computed by polynomial regression. More commonly, the distribution of the phase space is available from reconstructive methods [1], but knowledge about the coefficients is still desirable.

Alternatively this map can be used to describe a distortion from a desired phase space onto a measured one, to get insight into the distortion.

A Model for Symplectic Transfer Maps

Using the theory of Irwin [2] there is a simple way to parameterize an approximation $\mathcal{T}$ to a symplectic map $\mathcal{M}$. Using a series of kicks $\mathrm{K}_{c_n} := \exp(:g_n:)$, where g_n is a polynomial in x with coefficients c_n of degree P, $:\cdot:$ describes the Lie-operator and rotations R_Δ in the x-a-plane with a fixed angle Δ, the approximation $\mathcal{T}$, called Irwin model and defined as

$$\mathcal{T} := \mathrm{K}_{c_1} \circ \mathrm{R}_\Delta \circ \mathrm{K}_{c_2} \circ \mathrm{R}_\Delta \circ ... \circ \mathrm{K}_{c_k} \circ \mathrm{R}_{-\Delta}^k \circ \mathrm{R}_\varphi \approx \mathcal{M}$$

agrees up to order $P-1$ with the original map $\mathcal{M}$.

Finding the Map

The goal is to find a symplectic map which transforms the initial distribution described by a probability density p such that it fits to the measured data x_i. As the approximation is easily invertible, by changing the signs of the coefficients and angles and the order, it is much easier to find the most likely inverse map which transforms the measured data onto the distribution with a log-likelihood approach

$$\max_{c_1,\ldots,c_k,\varphi} \sum_i \log\left(p(\mathcal{T}^{-1}(x_i))\right).$$

With the high number of measurement points x_i and simple operations (polynomial evaluation, rotation, scaling), this minimization can easily be implemented by utilizing any modern machine learning framework and achieves sufficient performance for online evaluation. In this work, the PyTorch [3] framework and a stochastic gradient descend was used to maximize the likelihood. The transfer map in polynomial form was then computed by evaluating the model symbolically with SymPy [4].

Robustness

To improve the robustness of the optimization an initial rotation is added such that the first kick acts perpendicular to the angle with the highest normality, selected by performing the normality test [5] onto the measurement data projected onto an angle. This is combined with a sequential unfreezing of the parameters, such that the first kick, is also minimized first. This process is portrayed in Fig. 2: The leftmost panel shows an example phase space distribution, onto which the kick-layers are applied. The second panel shows the distribution after applying one optimized kick layer, which transforms the initial distribution closer to a normal distribution. After applying the full model, the distribution is shaped like a normal distribution. As normal distributions are rotational symmetric, it is impossible to detect rotation. To mitigate this effect partially, the four linear map components were encoded into Courant-Snyder parameters and emittance. The map was then rotated to be the identity matrix in first order, such that the map is decomposed into $\mathcal{T} = \mathcal{N} \circ \mathcal{L}$, where $\mathcal{L}$ is the linear part and $\mathcal{N}$ contains only the nonlinear part. This allows for better comparison on a by-coefficient base.

A More General Model

The required knowledge of the initial distribution can be reduced even further by prepending an affine linear map A to transform an ideal normal distribution, which transforms it into an arbitrary elliptic phase space. The affine map

$$A := B \circ \mathrm{R}_\theta \circ S$$

consists of a scaling S of the j-th coordinate by $1/s_j$, another rotation R with angle θ and a bias B, adding b_j to each coordinate. Then the generalized Irwin model $\mathcal{G}$ is defined as $\mathcal{G} := \mathcal{T} \circ A$ and the likelihood is calculated accordingly

$$\max_{c_1,\ldots,c_k,\varphi,\theta,s,b} \sum_i \log\left(p(\mathcal{G}^{-1}(x_i))\right) \cdot \prod_j 1/\left|s_j\right|.$$

Note that symplectic maps do not change the probability density, but an additional factor for the non-symplectic scaling operation is required.

This allows to separate a phase space into its linear components and the non-linear components applied afterwards, which give a much better description of the phase space as shown in the comparison in Fig. 1b.

APPLICATION TO FRS OPTIMIZATION

In the theory of ideal accelerators, each magnet affects the beam only in its order: Quadrupoles (QPs) govern all linear effects, sextupoles (SPs) the second order effects and so on. Determining the order of the deviation allows to split the optimization into per-order sub-problems, which are easier to solve. This enables the next step [6] in automatic optimization of the FRS [7].

Optimization Goal

At the dispersive focal plane of a fragment separator, the goal is to separate fragments by horizontal (x) position, which mostly depends on the momentum spread δ. Therefore all other contributions into the x-spot size must be small. While the magnification $(x|x)$ is limited by the geometry of the separator, the aforementioned and desired high momentum and angle spread turn the linear $(x|a)$ and quadratic $(x|aa)$ dependencies of the position to the angle into the major contributors, if they are not suppressed by precisely by the optics. Additionally decreasing the angular dispersion $(a|\delta)$ to zero, allows for parallel beam through the focal plane and a mirror symmetric layout which suppresses some higher order aberrations [8].

Experimental Setup

A 650 MeV u^{-1} $^{238}\mathrm{U}^{73+}$ beam was sent through a carbon foil to generate fully ionized, hydrogen-like and helium-like charge states of uranium, which enable simultaneous measurements of three different magnetic rigidities. The detector setup at fragment separators can determine single-particle coordinates at two positions near dispersive focal plane and thereby compute phase space coordinates for each particle. A pair of time projection chambers (TPCs) was used at FRS. To separate the measured positions into rigidites, the scikit-learn [9] clustering algorithm DBSCAN [10] separated the spots in the phase space, represented by the colors in Fig. 3. The estimated ratios of the particles in each spot were utilized to further improve the clustering by adapting the neighborhood distance parameter dynamically.

In contrast, the high beam intensity and high radiation environment at the FRS target during normal operation, prohibits particle by particle tracking, and so only limited information about the beam is available. To counteract this, the proposed generalized form of the transfer map was used.

Optimization

The algorithm was integrated into Geoff [11] and the robust and fast BOBYQA [12] algorithm was chosen as

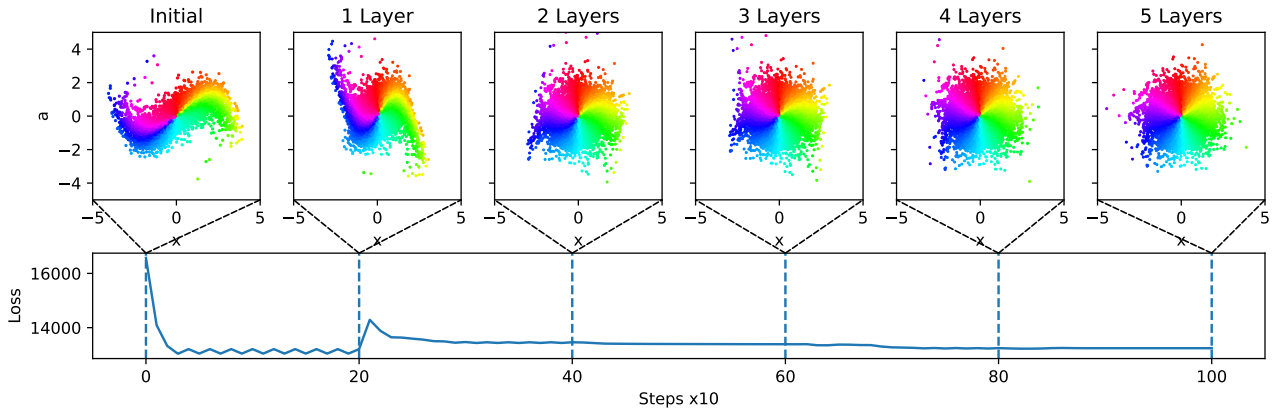

Figure 2: Layer-wise-optimization of the general Irwin model and its effect on a distorted distribution. The colors represent the angle in the final distribution.

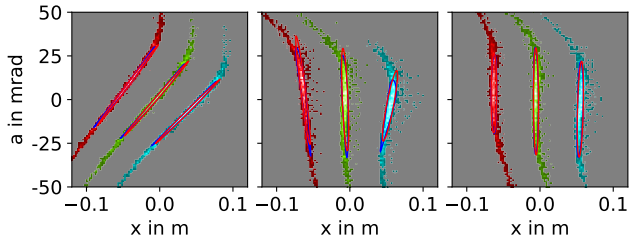

(a) Simulated FRS phase space. Initial, after QP optimization and after SP optimization.

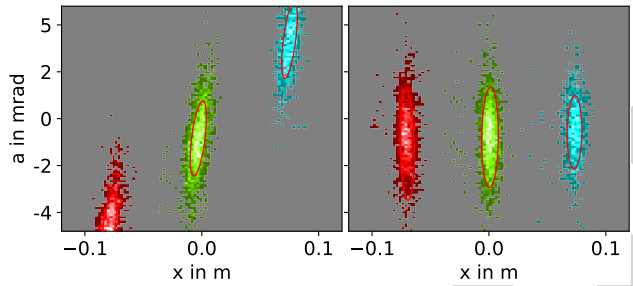

(b) Measured FRS phase space from TPCs. Initial and after QP optimization.

Figure 3: Phase space of the primary beam and its charge states (colors) at the dispersive focal plane.

optimizer. The verification of the method was performed in two scenarios: The FRS was simulated in COSY Infinity [13] and measurement data were computed. This simulation was connected to python and integrated into Geoff. This provided benchmarking and testing. Figure 3a shows that even with a strongly detuned setting, QP and SP optimization was possible. The remaining distortion is of third order and cannot be corrected with the available magnets. The second scenario was performed online with the real machine, magnets and detectors. Due to the modularity of Geoff this was possible with little changes of the code. The phase spaces in Fig. 3b show the intentionally detuned QPs and the focused and angular dispersion free setting, which was restored in 30 steps, performed in less than 5 minutes, as shown in Fig. 4.

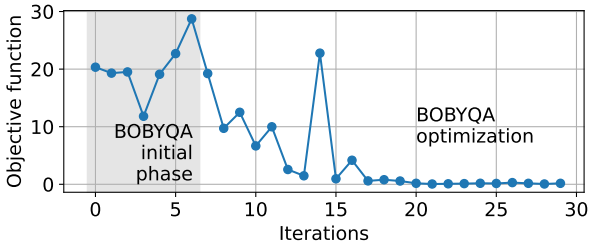

Figure 4: Loss function of the FRS optimization.

CONCLUSION

A new method based on symplectic theory and software was developed, which gives insight into nonlinearities of phase spaces. Having demonstrated its capabilities and optimization potential through both simulations and real-world machine operation, this method will be integral to the Super-FRS operation.

REFERENCES

[1] C. B. McKee, P. G. O'Shea, and J. M. J. Madey, "Phase space tomography of relativistic electron beams", *Nucl. Instrum. Methods Phys. Res., Sect. A*, vol. 358, no. 1, pp. 264–267, 1995. doi:10.1016/0168-9002(94)01411-6

[2] J. Irwin, "A multi-kick factorization algorithm for nonlinear maps", Lawrence Berkeley Lab., Berkley, CA, USA, Rep. SSC-228, Jul. 1989.

[3] A. Paszke *et al.*, "PyTorch: an imperative style, high-performance deep learning library", in *Proc. Int. Conf. Neural Inf. Process. Syst.* Red Hook, NY, USA: Curran Associates Inc., 2019.

[4] A. Meurer *et al.*, "SymPy: symbolic computing in Python", *PeerJ Comput, Sci.*, vol. 3, e103, Jan. 2017. doi:10.7717/peerj-cs.103

[5] R. B. D'agostino, A. Belanger, and R. B. D'Agostino Jr, "A suggestion for using powerful and informative tests of normality", *Am. Stat.*, vol. 44, no. 4, pp. 316–321, 1990.

[6] S. Appel *et al.*, "Automation of GSI key beam manipulations with AI methods", presented at HB'25, Huizhou, China, Oct. 2025, paper FRCAA01, unpublished.

[7] H. Geissel *et al.*, "The GSI projectile fragment separator (FRS): a versatile magnetic system for relativistic heavy ions", *Nucl. Instrum. Methods Phys. Res., Sect. B*, vol. 70, no. 1, pp. 286–297, 1992. doi:10.1016/0168-583X(92)95944-M

[8] H. Wollnik and M. Berz, "Relations between elements of transfer matrices due to the condition of symplecticity", *Nucl. Instrum. Methods Phys. Res., Sect. A*, vol. 238, no. 1, pp. 127–140, 1985. doi:10.1016/0168-9002(85)91037-X

[9] F. Pedregosa *et al.*, "Scikit-learn: machine learning in Python", *J. Mach. Learn. Res.*, vol. 12, pp. 2825–2830, 2011.

[10] M. Ester, H.-P. Kriegel, J. Sander, X. Xu, *et al.*, "A density-based algorithm for discovering clusters in large spatial databases with noise", in *Proc. KDD'96*, Portland, OR, USA, pp. 226–231, Aug. 1996.

[11] P. Madysa, S. Appel, V. Kain, and M. Schenk, "Geoff: the generic optimization framework & frontend for particle accelerator controls", *SoftwareX*, vol. 32, p. 102335, 2025. doi:10.1016/j.softx.2025.102335

[12] C. Cartis, J. Fiala, B. Marteau, and L. Roberts, "Improving the flexibility and robustness of model-based derivative-free optimization solvers", *ACM Trans. Math. Software*, vol. 45, no. 3, pp. 1–41, Aug. 2019. doi:10.1145/333851

[13] M. Berz and K. Makino, COSY INFINITY 10.2 Beam Physics Manual, 2023, https://www.bmtdynamics.org/cosy/manual/index.html